Influence of Structure on the Aseismic Stability and Dynamic Responses of Liquefiable Soil

Pengfei Dou
Beijing University of Technology
Chengshun Xu (xcs_2017@163.com)
Beijing University of Technology
Xiuli Du
Beijing University of Technology
Su Chen
Institute of Geophysics China Earthquake Administration

Research Article

Keywords: Free field, non-free field, shaking table tests, dynamic response, porewater pressure, seismic stability

Posted Date: March 16th, 2021

DOI: https://doi.org/10.21203/rs.3.rs-312945/v1

Version of Record: A version of this preprint was published at Bulletin of Earthquake Engineering on September 22nd, 2021. See the published version at https://doi.org/10.1007/s10518-021-01213-x.

Abstract

In previous major earthquakes, the damage and collapse of structures located in liquefied field which caused by site failure a common occurrence, and the problem of evaluation and disscusion on site liquefaction and the seismic stability is still a key topic in geotechnical earthquake engineering. To study the influence of the presence of structure on the seismic stability of liquefiable sites, a series of shaking table tests on liquefiable free field and non-free field with the same soil sample was carried out. It can be summarized from experimental results as following. The natural frequency of non-free field is larger and the damping ratio is smaller than that of free field. For the weak seismic loading condition, the dynamic response of sites show similar rules and trend. For the strong ground motion condition, soils in both experiments all liquefied obviously and the depth of liquefaction soil in the free field is significantly greater than that in the non-free field, besides, porewater pressure in the non-free field accumulated relately slow and the dissapited quikly from analysis of porewater pressure ratios(PPRs) in both experiments. The amplitudes of lateral displacements and acceleration of soil in the non-free field is obviously smaller than that in the free field caused by the effect of presence of the structure. In a word, the presence of structures will lead to the increase of site stiffness, site more difficult to liquefy, and the seismic stability of the non-free site is higher than that of the free site due to soil-structure interaction.

Introduction

As early as 1964, during the Alaska earthquake in USA and the Niigata Earthquake in Japan, the foundation bearing capacity reduction, uneven settlement and lateral spreading caused by soil liquefaction lead to the overturning and collapse of structures observed in the post-earthquake investigation. In previous major earthquakes, foundation failure due to liquefaction of sand and soil was observed, resulting in the destruction of buildings caused by then. Liquefied soil-structure dynamic system damaged under seismic loadings is not only related to the dynamic characteristics of soil or the structure, but also related to the change of mechanical properties of sand soil after liquefaction, the deformation behaviors at the contact surface of soil and structure as well as the transfer mechanism of interaction forces. Therefore, the problems of soil-structure dynamic interaction under seismic loadings should be more complicated involving the liquefaction of saturated sand. Study on soil liquefaction under seismic loadings is still an important research topic in geotechnical earthquake engineering [1], and many scholars have carried out a large number of studies on the liquefaction possibility discrimination of saturated sandy soil, liquefied soil-structure dynamic interaction and foundation failure of liquefied site by means of numerical calculation model [2–5], various experimental techniques [6–11] and theoretical method an analysis [12–16], and the seismic responses of various structures in liquefaction site were discussed in detail.

The evaluation of liquefaction possibility and risk as well as the discussion of soil-structure dynamic interaction are the main aspects of scientific problems related to liquefaction. In the aspect of liquefaction identification, global numerical models of liquefiable site-structure system are established by using finite element method, finite difference method and other numerical analysis methods, and it is an

efficient method to evaluate the liquefaction possibility of saturated sandy soil via the simulation results of the numerical analysis model. The numerical analysis model can consider soil-structure interaction, and the development of porewater pressure, stress and strain as well as dynamic responses of soil liquefaction process. However, liquefaction probability analysis of site soil from the numerical model depends on the choice of liquefied soil dynamic constitutive model and the reliability of various physical parameters in this model also have high requirements.

In the liquefaction discrimination method based on the field investigation data, the liquefaction possibility analysis is generally not considered for the free site (i.e. the site without any structure) and the influence of structures to be constructed or the buildings and structures nearby is not considered [17]. In fact, when there is any building in sites, due to soil-structure interaction, the dynamic stress state and drainage conditions of soil under dynamic loadings are obviously different from those in a free site. Therefore, it is difficult to proceed with accurate assessment of the liquefaction possibility and to predict seismic responses of saturated sand in the non-free site. Actually, the accurate assessment of the liquefaction possibility of saturated sand is related to the following analysis and correct understanding on the site stability of the building foundation under seismic loadings. In previous studies, most dynamic catastrophe process studies involving liquefied soil-structure dynamic system under seismic loadings just focused on the earthquake response of superstructures as a research expatiates [18–22], or analyzed and discussed soil liquefaction mechanism and site failure as well as liquefaction spreading problems only from the perspectives on the soil liquefaction features or seismic responses of the free site [23–28]. There are few experimental studies on the influence of the existence of structures on the evaluation of liquefaction possibility and seismic stability.

As a reliable research method of geotechnical engineering, shaking table test technology has been widely used in studying on the problems of soil-structure dynamic interaction, seismic response of liquefaction site, etc. Especially involving the problem on sandy soil liquefaction, using the use of shaking table test technology can effectively avoid the problems of any influence on seismic response of liquefiable fields from the selection of constitutive model of liquefied soil and the simulation of soil-structure interface in a numerical model analysis. In this paper, two groups of large shaking table tests are carried out for discussing on the influence of the structure on the seismic stability of liquefiable sites. By comparing the experimental results from the free field and non-free field experiments, such as the dynamic characteristics, acceleration response, the rules of porewater pressure ratios in saturated sand layer, soil lateral displacements, etc., the influence of the existence of the structure on the dynamic characteristics and seismic stability of the liquefiable site is analyzed and summarized.

1 Description Of Shaking Table Test

The contents of experimental design scheme, include the chosen shaking table, similar ratio design, laminar shear soil container, etc., have been introduced in Reference [29, 30] in detail. In order to facilitate understanding of the test results analysis in this paper, in the following introduction of the test scheme,

only the model system setting, sensor layout, loading conditions and other contents are introduced as necessary.

Figure 1 presents a schematic drawing of the whole test package for the pile group-superstructure in either the free field or the non-free field on the shaking table. In this series of shaking table experiments, the model sites are all consisted of the same stratified soils, with 0.5m dense sandy soil layer, 1.2m loose sand layer (i.e. saturated sandy soil layer) and 0.3m clay crust layer, successively from bottom to top. The pile group consisted of four piles placed in a 2×2 configuration, and the superstructure is a simplified structure composed of two lumped masses. The natural vibration frequency of the structure is approximately 0.7s.

Live-action on shaking-table in Experiment-NF is shown in Fig. 2. Figure 3 is layout of test package and instrumentation in both experiments.

In this series of shaking table experiments, a sine beat wave with the acceleration amplitude of 0.05g and the Wolong seismic record in Wenchuan Earthquake with the amplitude of 0.3g are selected as the ground motions. White noise is chosen to obtain the dynamic characteristic of model system before and after tests. The sine beat wave curve and the time history and corresponding Fourier spectrum of Wolong seismic record are displayed in Figs. 4 and 5.

2 Dynamic Characteristic Of Model Systems

Before and after inputting seismic records, white noise with the amplitude of 0.05g was inputted to sweep the frequency of model system, and the natural frequencies and damping ratios of model systems in both experiments were obtained as listed in Table 1. It should be noted that the dynamic characteristic of soils in both experiments were paid attention to, so the frequencies and damping ratios are all calculated from the data measuring by SAA2.

As shown in Table 1, the natural frequencies of the model system obtained from the second white noise sweep (before the test) were smaller than that from the first white noise sweep (after the test), while the damping ratio is increased after the end of ground motions exciting.

The dynamic characteristics of non-free field and free field are different to some extent: due to the existence of structures made of materials with large stiffness, the natural frequency of free field is lower than that of non-free field, while the damping ratio of free field is higher than that of non-free field. The natural vibration frequency of the non-free field is large, but the damping is small, which indicates that the stiffness of the field will be increased and the energy dissipation capacity will be decreased to some extent in the presence of the structure.

Table 1
Dynamic characteristics of model system in Experiment F and Experiment NF

Test events	Basic frequency		Damping ratio	
	Free field	Non-free field	Free field	Non-free field
White noise (before shaking test)	4.85Hz	5.43Hz	4.2%	3.9%
White noise (after shaking test)	4.52Hz	4.84Hz	5.4%	4.2%

3 Soil-structure Interaction In The Non-free Field

In the non-free field experiment, SAA1 and SAA2 were used to measure the acceleration response of the pile and soil, respectively. Actually, the soil-structure dynamic interaction reflected in acceleration responses is that there are the differences in peak values of acceleration waveform and corresponding response spectrum. Figure 6 and Fig. 7 display the acceleration time histories and corresponding spectra of 0.3g Wolong ground motion record measuring by SAA1 and SAA2. It can be seen from the figures that the time-history waveforms and amplitudes of acceleration response of pile and soil at the same depth are different, and the response spectrum curves of corresponding measuring points are also obviously distinguishing. That is, the vibration of pile and soil is not consistent, and there is a phase difference between them, which indicates that the soil-structure dynamic interaction is very strong.

4 Porewater Pressure Responses

4.1 Porewater pressure development

According to the porewater pressure data obtained from each measuring point, all of the porewater pressure ratios(PPRs) at different positions can be calculated, and then peak porewater pressure color nephograms were drawn in the software Surfer (Version 12.0). It's important to point out herein, that the porewater pressure sensors at W3 and W6 is damaged in Experiment-F and the porewater pressure sensor at W14 is damaged in Experiment-NF. Figure 8 and 9 display the peak porewater pressure color nephograms of saturated sand layer for 0.05g sine beat wave and 0.3g Wolong seismic record in both experiments.

As shown in Figure 8, porewater pressure ratios in saturated sand layer are all very small in both experiments for the test case of 0.05g sine beat wave. The porewater pressure ratios in the upper of saturated sand layer are maximum and reach or close to 0.3. In fact, except the area near measuring point W7, the values of porewater pressure ratio at different positions are very close, and that is, the presence of the structure has little effect on the overall pore pressure reaction under the weak seismic loading.

Figure 9 illustrates the peak porewater pressure color nephograms 0.3g Wolong seismic record, and the areas with pore pressure ratios greater than 0.8 has been circled by the dotted line. In both experiments,

the peak porewater pressure ratios at measuring points W1 and W2 in the saturated sand layer are all smaller than that at other measuring points with the same height, which is caused by the gaps between soil and the container. By comparing Figure 9a and b, it can be seen that the peak porewater pressure ratios at the same depth in the free field is slightly higher than that at the corresponding depth in the non-free field, and the liquefied soil area in the free field is significantly larger, that is, the liquefaction depth of the saturated sandy soil layer in the free field is deeper. The main reason for the differences is caused by the gaps due to the detachment and slippage between soil with piles and the cap during the strong vibration process, and the next section will continue the analysis at the viewpoint of pore pressure time history. In fact, the detachment and slippage should be caused by the vibration phase difference between pile-structure system and soil as the rule summarized from Figure 9.

There are so many porewater pressure sensors embedded in the saturated sand layers, that the data measuring by the sensors located in the area with high porewater pressure ratios were analyzed herein, i.e. at the measuring points W4, W5, W7, W8, W12 and W13. The time histories of porewater pressure ratio at the six measuring points were illustrated in Figure 10, 11 and 12.

From the porewater pressure responses at measuring points W4 and W5 far from the structure or the center of soil as shown in Figure 10, the time history waveforms and amplitudes of PPRs in this area are similar, and it shows that the pore pressure development of the non-free field is similar to that of the free field in fact. For the porewater pressure responses at the others measuring points as shown in Figure 11 and 12, in the non-free field test, porewater pressure accumulation at the measuring points W7, W8, W12 and W13 close to the structure in the period from 5s to 13s were at a low level and did not reach the peak porewater pressure ratio around the tenth second respectively. In the free field, the accumulation rates of porewater pressure are all faster than that of each pore pressure measuring point near the soil center. Compared with the pore pressure ratios at the same positions in the non-free field, the pore pressure ratio in the free field was generally higher at about 12s. That is, during the period with strong shaking, the developments of pore pressure ratio are obviously affected due to the existence of structure, and it is difficult for the pore pressure ratio to reach a higher level in a short time.

For the time histories of pore pressure ratio after 35s at each measuring point, it can be seen that the dissipation rates of pore pressure near the structure in the non-free field is obviously faster than that at the same positions in the free field, and the pore pressure ratios in the free field will stay at a very high level for a long time without obvious dissipation. Quantitative analysis of this is carried out in the following section.

It should be noted that the " waterspouts and sand boils " phenomenon was exhibited at the upper part of the measuring point W7 during the test, so the time-history curve of the pore pressure ratio at the measuring point W7 suddenly decreased obviously to a smaller value when it was 10s-20s.

On the whole, in the Experiment-NF, the pore water pressure ratios near the structure is relatively small, and there is no rapid accumulation of porewater pressure due to soil-structure dynamic interaction. The main reasons should be that there are gaps in the interface between soil and structure since they are

separated and slipped during the strong vibration process. In this series of shaking table tests, the structure system includes a pile-group foundation, so the pore water near the structure can dissipate upward through the contact surface between soil and the pile foundation and the pore water pressure is difficult to accumulate rapidly in the period of strong vibration. In fact, a large amount of water began to appear around the pile cap at about 15s in the tests. Furthermore, there is no structure in the Experiment-F, and the upper layer is covered by a 0.3m thick clay layer, so the porewater pressure cannot dissipate in a short time, even stays at a very high level for a long time after the end of the vibration loading.

4.2 Quantitative analysis on porewater pressure dissipation

Some studies [31-35] discussed the effect of the shaking duration and seismic energy on liquefaction, and held the views that the duration of shaking should be an important and relevant parameter affecting soil liquefaction and porewater pressure would accumulate with increase of the energy of ground motions. In fact, for the duration of strong ground motion, many definitions of it based on seismic energy have been elucidated in some previous literatures. The definition of the duration of strong ground motion suggested by Trifunac and Brady [36] is called significant duration, which defined by the time required for the energy of the ground motion to reach 5% to 95% of the total energy. This definition is mentioned and used herein for discussing the accumulation and dissipation of porewater pressure correlated with shaking energy of seismic loadings. For the seismic ground motion record measuring at the shaking table, i.e. at the measuring point X0t, the timing of reaching 5% total energy of the ground motion is at 7.55s and that of reaching 95% is at 21.29s as pointed at Figure 13, and the significant duration is 13.74 seconds. As displaying in Figure 10, 11 and 12, the peak porewater pressure ratios at different measuring points are all near the timings of acceleration peak amplitude or that of reaching 95% total energy of the ground motion. In particular, porewater pressure ratios keep at a high level in the period of the significant duration. The porewater pressure ratios at different timings are listed in Table 2. It should be noted that there are several specific timings were paid an attention to herein. The timing at the outset of strong shaking marks the beginning of steep accumulation of porewater pressure and PPRs at each measuring point increase obviously in the period from 7.55s to 21.29s as shown in Table 2. In addition, the acceleration amplitudes and the shaking energy are all very small after 25s, so the porewater pressure should show the of trend of dissipation from this timing. The dissipation rates of porewater pressure in the period from 25s to the end of recording porewater pressure time-histories were calculated in Table 2 and discussed as following.

As listed in Table 2, in the free field, the PPRs at the end of the seismic loading are all close to the corresponding peak PPR values at each mearing point. It shown that PPR dissipation rates at the measuring points in the free field are all small, except at W4. PPRs at several measuring points such as W8 and W12 increased slightly comparing with that at the time point 25s, and this suggests that the pore pressure ratios in free-field soil still keep at a high level for a certain time after the strong shaking period with high seismic energy and the development of porewater pressure even shows an accumulation trend.

For the PPR dissipation rates in non-free field listed in Table 2, the porewater pressures at each measuring point dissipated obviously from 25s to 60s, and except that at W5, all of PPR dissipation rates reach around 20%. PPR dissipation at liquefied area in non-free field are significantly faster comparing with that in the free field.

The distance between measuring points W4, W5 and the pile is about 6.5 times the pile diameter as illustrated in Fig.3. In fact, it also shown that the range of influence of structure on PPR in the liquefied site is very large from the discussion on the rules of PPR at W4 and W5. In this series of shaking table tests, it is no doubt that the PPR data measuring at W1, W2 and W3 were affected by the soil boundary, on account of porewater pressure dissipated from the surface between soil and the rubber membrane attached to the soil container. Therefore, the rules of PPR at W4 and W5 reflect that the distance of the structural influence on the liquefied site was at least 6.5D away from the pile-group, from qualitative point of view.

Table 2 Porewater pressure at different timings and PPR dissipation rate at upper measuring points

Test scheme	Measuring Point	Peak PPR	7.55s (5%)	21.29s (95%)	25s (97.8%)	80s (At the end)	PPR dissipation rate
Free field	W4	0.96	0.09	0.93	0.95	0.83	12.06%
	W5	0.66	0.00	0.55	0.59	0.61	-3.62%
	W7	1.00	0.13	0.80	0.77	0.81	-5.30%
	W8	1.00	0.04	0.95	0.98	0.98	0.35%
	W12	1.00	0.04	0.98	0.96	0.89	7.14%
	W13	1.00	0.01	0.85	0.91	0.96	-5.82%
Non-free field	W4	1.00	0.08	0.99	0.97	0.77	20.78%
	W5	0.77	0.00	0.59	0.65	0.58	9.75%
	W7	1.00	0.04	0.91	0.92	0.75	18.33%
	W8	0.94	0.04	0.89	0.93	0.71	23.31%
	W12	1.00	0.02	0.95	0.99	0.76	23.47%
	W13	0.75	0.03	0.69	0.74	0.55	24.95%

5 Acceleration And Response Spectra

The acceleration amplification factor is the ratio of the peak acceleration at the measuring point to the peak acceleration of inputting seismic record at the bottom of the soil mass. The magnitude of the acceleration amplification factor indicates the amplification or damping effect of the soil on the seismic loadings. The acceleration data measured at each measuring point of SAA2 were used to calculate the acceleration amplification factor of soil mass in both experiments. Figure 14a and b show the distribution diagram of the acceleration amplification factor of soil mass when 0.05g sinusoidal beat wave and 0.3g Wolong seismic record were input, respectively.

For the test case with 0.05g sine beat wave, the acceleration responses of saturated sand layer and clay layer in both experiments showed a trend of continuous amplification from the bottom to soil surface and the acceleration amplification factor of the upper soil reached 2, which indicated the soil mass had an obvious amplification effect on the seismic loading. Moreover, the acceleration amplification factor of soil mass of the non-free field is slightly larger than that of the free field. But from the overall trends, the acceleration amplification factor of soil mass in both experiments differs little from each other. This shows that the existence of the structure has no obvious influence on the acceleration amplification effect of the soil under the weak seismic vibration.

For the test case with the 0.3g Wolong seismic record, the soil in both experiments all had no obvious amplification effect on the earthquake loading except for the topmost clay layer, but the magnitude and trend of acceleration amplification factor were significantly different. In the Experiment-F, the acceleration response at the lower part of the saturated sand layer has a certain decrease, while the upper part of saturated sand layer has a small amplification effect on the earthquake loading. The acceleration amplification factor at the clay layer even reaches 1.52, which the acceleration response is significantly amplified here. For the Experiment-NF, acceleration amplification factor at each measuring point in soil mass is less than 1, and it shows that the acceleration response has no amplification at all positions in soil. Moreover, the acceleration amplification factor in the middle and upper part of saturated sand layer and in the clay layer is obviously lower than that in the corresponding positions in the free field, which indicates that the existence of the structure significantly reduces the acceleration response of the field.

Figure 15 shows the acceleration response spectra corresponding to each SAA2 measurement point in both experiments with the test case with 0.3g Wolong earthquake record. It can be seen from Figure 15 that the acceleration response spectra at SAA2-1 in the dense sand layer in both experiments are very close to that of the input seismic record, and only part of the high-frequency components (which with period less than 0.1s) are filtered, which is due to the high stiffness of the dense sand layer and SAA2-1 measurement point is near the bottom of the soil. In addition to the measuring point in the dense sand layer, the response spectra at the other measuring points in the free field are very different from that of the input seismic record. Long-period components with a period greater than 0.15s will be amplified to some extent, especially the reaction acceleration amplification near 0.2s (corresponding the frequency 5Hz) is obvious. Compared with the response spectrum of the input seismic record, the acceleration response spectra of the measured points in the non-free field has almost the same, and the periodic components have no significant change.

Combining with the analysis on acceleration amplification factors, it can be summarized that the structure obviously changed the characteristic of the seismic loadings propagating in soil, and the amplitudes and periodic components of acceleration signals of the field change greatly due to the existence of the structure. Soil mass of the free field may have a certain amplification effect on seismic load and will enrich the long period ground motion components. In the non-free field, due to the soil-structure dynamic interaction, the peak values of acceleration decrease obviously in the field and its periodic components have no significant change. In the Experiment-NF, due to the far distance between SAA2 and the structure, and the liquefaction of the soil, the first two natural frequencies of the structure (corresponding to periods 0.7s and 0.09s) have no significant influence on the acceleration response spectra of soil.

6 Lateral Displacement Of Soils

The lateral deformation of the soil can be measured and calculated by the inclinometers in SAA. Figure 16a and b respectively show the distribution diagram of the lateral earth displacement amplitudes obtained by SAA2 for the test cases with 0.05g beat wave and 0.3g Wolong earthquake record in both experiments.

As shown in Fig. 16a, it can be found that the lateral deformation rule of soil in the free field is consistent with that in the non-free field, which is that the lateral displacements at the upper soil are all large and lateral displacements at the lower part of soil mass are small and almost the same. In the free field, the lateral displacement amplitudes of all of the soil are much larger than that in the non-free field. The lateral displacements of the soil in the free field is 5mm-6mm larger than that in the non-free field. The lateral displacement of the clay layer and the upper part of saturated sand layer in the free field is 12-14mm, while the maximum lateral displacement at the same position in the non-free field is only 5-7mm.

Figure 16b shows the distribution of lateral displacement amplitudes of soil for the test case with the 0.3g Wolong earthquake record, and the soil displacements for the test case with the 0.3g Wolong earthquake record was significantly greater than that for the test case with the 0.05g beat wave as illustrated in Fig. 16a and b. The lateral displacements of the non-free field soil are about 10mm to 15mm, and the lateral displacement amplitudes of soils, except at the measured point in the dense sand layer, are all 40mm approximately. Due to the existence of structure in the non-free field, the lateral displacement of the soil at each measuring point from top to bottom differs little. In the free field, the lateral displacement of the soil in the dense sand layer is the smallest and that at the lower part of the saturated sand layer is the largest, and it shows the rule with the amplitudes from the bottom up varied from small to large and then decreased. It should because the stiffness of the dense sand layer is large, so the deformation is small. The lateral displacement of the lower part of the saturated sand layer is large due to the possible relative sliding at the interface of the soil layers as well as the small soil stiffness, and the vibration isolation effect of clay layer and the upper part of saturated sand due to soil liquefaction, it causes that the lateral displacements in the middle and upper soil layer is smaller than that in the lower

soil. To sum up, the existence of the structure significantly reduces the lateral displacement response of the field soil.

Combined with the results of acceleration and porewater pressure response in both experiments above, it can be seen that the existence of pile group-superstructure system reduces the dynamic response of the surrounding liquefiable soil and significantly improves the aseismic stability.

7 Conclusions

It is no doubt that this series of shaking table experiments is qualitative one and proceeding precise quantitative analysis based on the data from shaking table tests to reflect the rules of any prototype site is difficult, and quantitative and further analysis on more problems such as the influence range of the pile-group on the development of porewater pressure in liquefied soil calls for refined numerical model to research. The conclusions summarized from experimental results still provides important reference for liquefaction analysis.

By comparing the experimental results of the free field and non-free field experiments, the differences of soil acceleration, porewater pressure and lateral displacement between the test groups of free field and non-free field were discussed and analyzed, and the experimental results shown that the dynamic characteristics, seismic responses and aseismic stability of the soil are all obviously distinguishing caused by the existence of structure. The existence of a structure actually will reduce the seismic responses of the liquefiable site and is beneficial to improving the aseismic stability of the field with liquefiable sandy soil layer. In addition, it also suggests that substructure analysis method used in the study of soil-structure dynamic response may underestimate the aseismic stability of the field soil, due to the extracted free field response obviously greater than that of the ground around the actual structural system, and cause that the calculated result will differ greatly from the real responses. The main conclusions are as followings:

1. For the weak seismic loading condition, the rule of porewater pressure ratio is similar in both experiments. During strong shaking process, the porewater pressure near the structure accumulated more slowly and PPR is hard to reach a higher level in a short time in the non-free field. In the free field, the saturated sand is more prone to liquefaction and the depth of liquefaction is also larger. This rule indicates that soil-structure dynamic interaction have obvious influence on the development of field liquefaction, and cause the liquefiable sand layer harder to liquefy.
2. After strong shaking, the porewater pressures dissipate more rapidly in the non - free field, especially that near the structure. The existence of the structure affects the dissipation rate of porewater pressure significantly, which also shows that the structure not only have an influence on the accumulation of porewater pressure, but also big effects on the dissipation rate of that.
3. Compared with seismic responses of the free field, the acceleration response and lateral displacement of soil in the non-free field are significantly smaller, which indicate that the existence of

the structure weakens the dynamic response of soil obviously. That is, the field is less likely to fail and the aseismic stability is improved.

4. The influence range of the structure on the seismic response of soil such as acceleration and the development of porewater pressure as well as lateral displacement of soil reaches 6.5 times the pile diameter at least.

Declarations

We would like to submit the enclosed manuscript entitled " Influence of structure on the aseismic stability and dynamic responses of liquefiable soil", which we wish to be considered for publication in Bulletin of Earthquake Engineering.

This work was supported by the Foundation for Innovative Research Groups of the National Natural Science Foundation of China (Grant No.51421005), the National Natural Science Foundation of China (Grant No.51578026) and the National Science Fund for Excellent Young Scholars of China (Grant No.51722801).

All of authors declare that they have no known competing financial interests or personal relationships that could have appeared to influence the work reported in this paper. All authors named in the paper have participated in this work and agreed for the manuscript to be submitted to BEE.

All of the data and material in the manuscript are available from the corresponding author.

References

1. National Research Council (1985) Liquefaction of soils during earthquakes[R]. National Academy Press, Washington D C
2. Li Gangjin R, Motamed (2017) Finite element modeling of soil-pile response subjected to liquefaction induced [J]. Soil Dynamic Earthquake Engineering 92:573–584
3. Qiu Zhijian Lu, Jinchi E, Ahmed et al (2019) OpenSEES Three-Dimensional Computational Modeling of Groud-Structure Systems and Liquefaction Scenarios. Computer Modeling in Engineering Sciences 120(3):629–656
4. Lu Jinchi E, Ahmed Y, Linjun et al (2011) Large-Scale Numerical Modeling in Geotechnical Earthquake Engineering. Int J Geomech 11(6):490–503
5. Mokhtar A, Abdel-Motaal M, Wahidy M (2014) Lateral displacement and pile instability due to soil liquefaction using numerical model. Ain Shams Engineering Journal 5:1019–1032
6. Haeri S, Kavand A, Rahmani I et al (2012) Response of a group of piles to liquefaction-induced lateral spreading by large scale shake table testing. Soil Dyn Earthq Eng 38:25–45
7. Motamed R, Towhata I et al (2009) Behavior of pile group behind a sheet pile quay wall subjected to liquefaction-induced large ground deformation observed in shaking test in E-defense project. Soils

Found 49(3):459–475

8. Tabata K, Sato M. E-Defense Shaking Table Test on the Behavior of Liquefaction-Induced Lateral Spreading of Large-Scale Model Ground with a Pile-Foundation Structure Behind Quay Wall [C]//International Conferences on Recent Advances in Geotechnical Earthquake Engineering and Soil Dynamics, 2010,1–6
9. Suzuki H, Tokimatsu K, Sato M et al. Factor Affecting Horizontal Subgrade Reaction of Piles during Soil Liquefaction and Lateral Spreading [C]//Workshop of Seismic Performance and Simulation of Pile Foundations in Liquefied and Laterally Spreading Ground: University of California, Davis, California, 2005(3):16–18
10. Lei Su, Liang T, Xianzhang L et al (2015) Responses of reinforced concrete pile group in two-layered liquefied soil-shake-table investigations. Journal of Zhejiang University Science A 16(2):93–104
11. Gao X, Ling X, Tang L et al (2011) Soil–pile–bridge structure interaction in liquefying ground using shake table testing. Soil Dyn Earthq Eng 31(10):9–17
12. El Naggar MH, Novak M (1994) Non-linear model for dynamic axial pile response. Journal of Geotechnical Engineering 120(2):308–329
13. El Naggar MH, Novak M (1994) Nonlinear lateral interaction in pile dynamics. Soil Dyn Earthq Eng 14:141–157
14. Elsawy MK, El Naggar MH, Cerato AB et al (2019) Data reduction and dynamic p-y curves of helical piles from large-scale shake table tests. Journal of Geotechnical Geoenvironmental Engineering ASCE 145(10):04019075
15. Boulanger RW, Curras CJ, Kutter BL et al. Seismic Soil-pile-structure interaction experiments and analysis. Journal of Geotechnical Geoenvironmental Engineering, ASCE 1991,125(9): 750–759
16. Varun AD (2012) A generalized hysteresis model for biaxial response of pile foundations in sands. Soil Dyn Earthq Eng 32:56–70
17. Du, XiuLi (2011) Lu DeChun. Advances in soil dynamics and geotechnical earthquake engineering. Rock Soil Mechanics 32(S2):10–20
18. Chen Guoxing C, Chengzhi SQ et al (2015) Shaking table tests on a three-arch type subway station structure in a liquefiable soil. Bull Earthq Eng 13(6):1675–1701
19. Motamed R, Towhata I (2010) Shaking table model tests on pile groups behind quay walls subjected to lateral spreading. Journal of Geotechnical Geoenvironmental Engineering ASCE 136(3):477–489
20. Motamed R, Towhata I (2010) Mitigation measures for pile groups behind quay walls subjected to lateral flow of liquefied soil. Soil Dyn Earthq Eng 30:1043–1060
21. Motamed R, Sesov V, Towhata I et al (2010) Experimental modeling of large pile groups in sloping ground subjected to liquefaction-induced lateral flow 1-g shaking table tests. Soils Found 50(2):261–279
22. Hayashi K, Kaneda S (2019) Nonlinear response and damage monitoring of a concrete pile as a result of soil liquefaction. Structural Engineering International 3:370–376

23. Varghese R, Latha G. Shaking Table Studies on the Conditions of Sand Liquefaction[C]//Geo-Congress 2014 Technical Papers, 2014(234):1244–1253
24. El Shamy U, Zeghal M, Dobry R et al (2010) Micromechanical aspects of liquefaction-induced lateral spreading. Int J Geomech 10(5):190–201
25. Tsai CC, Lin WC, Chiou JS (2016) Identification of dynamic soil properties through shaking table tests on a large saturated sand specimen in a laminar shear box. Soil Dyn Earthq Eng 83:59–68
26. Hadush S, Yashima A, Uzuoka R (2000) Importance of viscous fluid characteristics in liquefaction induced lateral spreading analysis. Comput Geotech 27(3):199–224
27. Sasaki Y, Towhata I, Tokida K et al (1992) Mechanism of permanent displacement of ground caused by seismic liquefaction [J]. Soil Foundations 32(3):79–96
28. Ye B, Yokawa H, Kondo T et al (2006) Investigation on Stiffness Recovery of Liquefied Sandy Ground after Liquefaction Using Shaking-Table Tests [C]// Proceedings of Sessions of GeoShanghai: Pavement Mechanics and Performance. Reston, Virginia, U.S.A., ASCE PRESS, 482–489
29. Xu CS, Dou PF, Du XL et al. Seismic performance of pile group-structure system in liquefiable and non-liquefiable soil from large-scale shake table tests. Soil Dynamics and Earthquake Engineering. doi.org/10.1016/j.soildyn.2020.106299
30. Xu CS, Dou PF, Du XL et al. Large shaking table tests of pile-supported structures in different ground conditions. Soil Dynamics and Earthquake Engineering. https://doi.org/10.1016/j.soildyn.2020.106307
31. Davis RO, Berrill JB (1982) Energy dissipation and seismic liquefaction in sands. Earthquake Eng Struct Dynam 10(1):59–68
32. Berrill JB, Davis RO (1985) Energy dissipation and seismic liquefaction of sands: revised model. Soils Found 25(2):106–118
33. He Guangna (1981) Energy analysis procedure for evaluating soil liquefaction potential. Chinese Journal of Geotechnical Engineering 3(4):11–21
34. Guo Ying H (1992) Guangna. Relationship between dynamic pore pressure and excited energy of light loam and its application to predicting site liquefaction potential. Journal of Dalian University of Technology 32(6):732–736
35. Xu Chengshun D, Pengfei G, Liucheng, et la. Shaking table test on effects of ground motion duration compression ratio on seismic response of liquefied foundation. Rock and Soil Mechanics, 2019, 40(1): 147–155
36. Hancock J, Bommer JJ (2007) Using spectral matched records to explore the influence of strong-motion duration on inelastic structural response [J]. Soil Dyn Earthq Eng 27:291–299

Figures

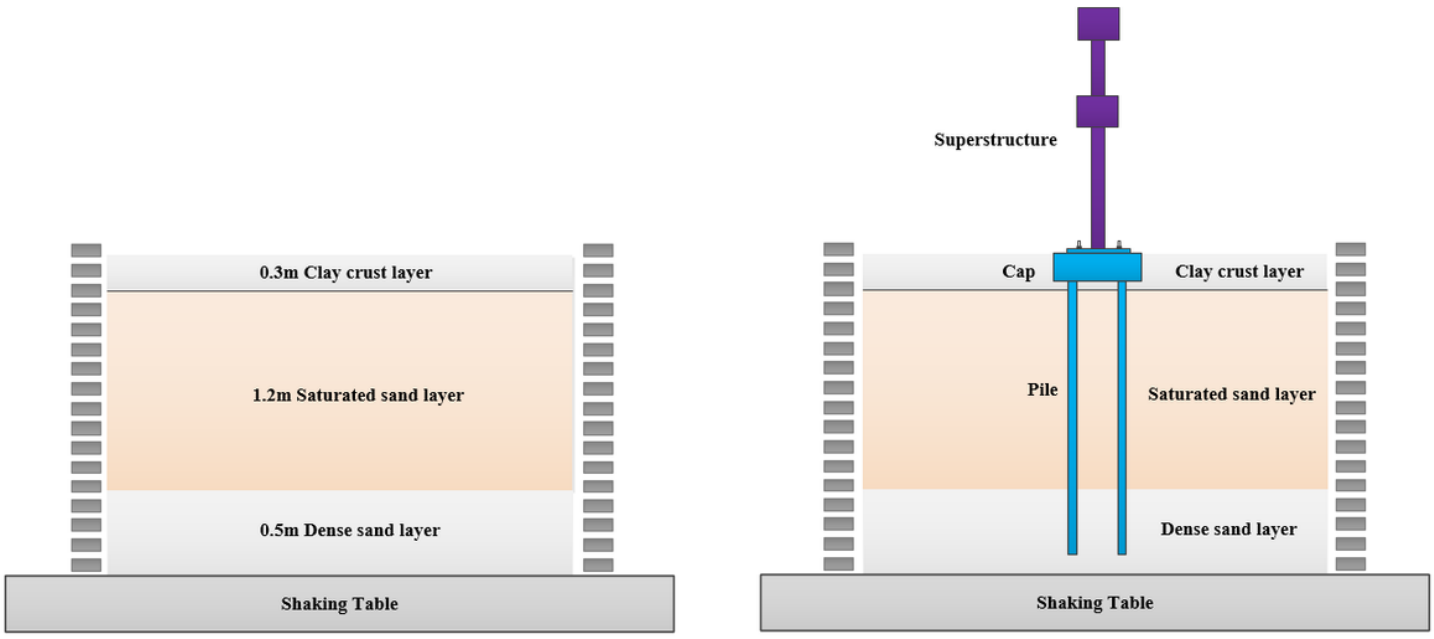

Figure 1

Model systems in two experiments: a) Experiment-F; b) Experiment-NF

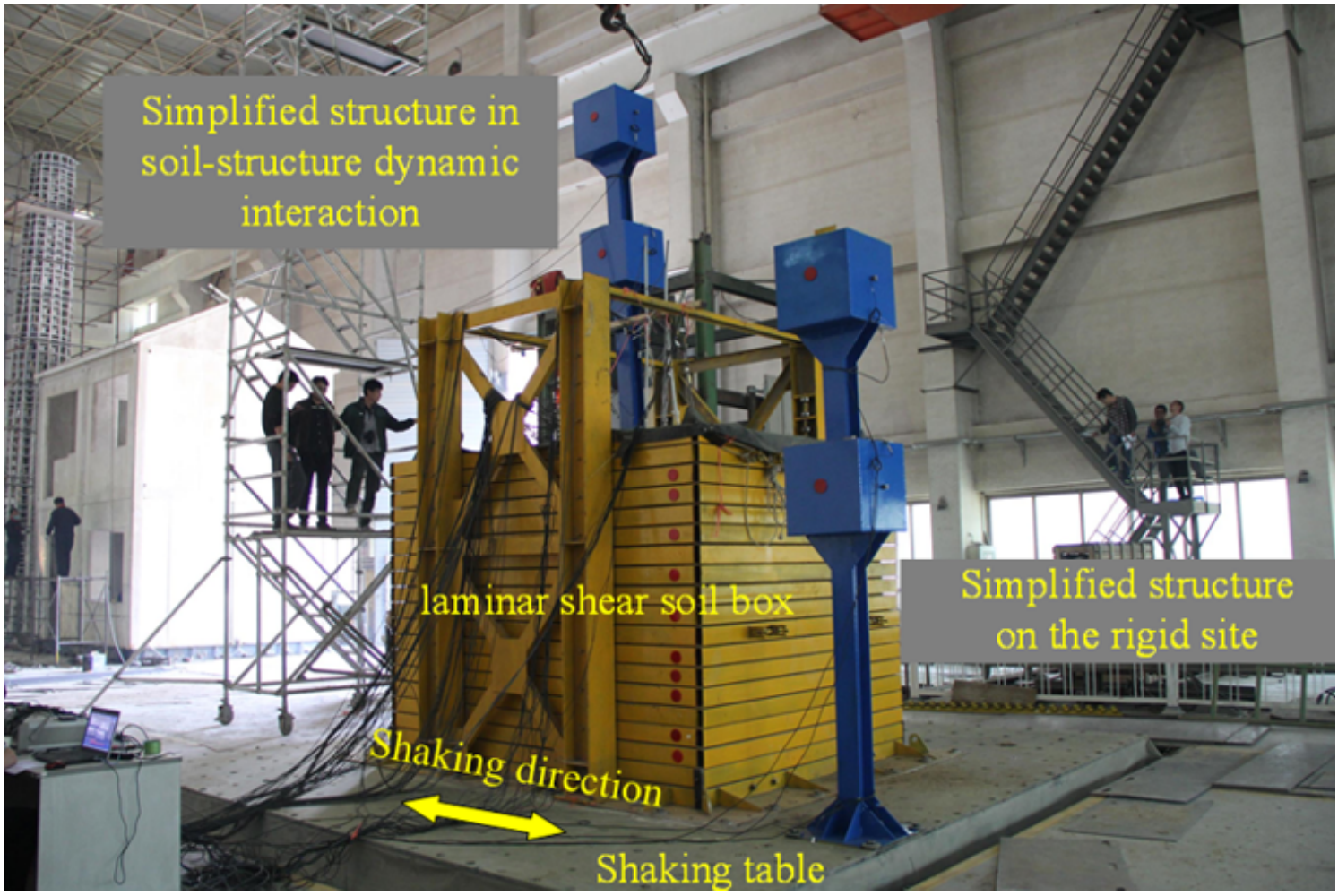

Figure 2

Live-action on shaking-table in the Experiment-NF

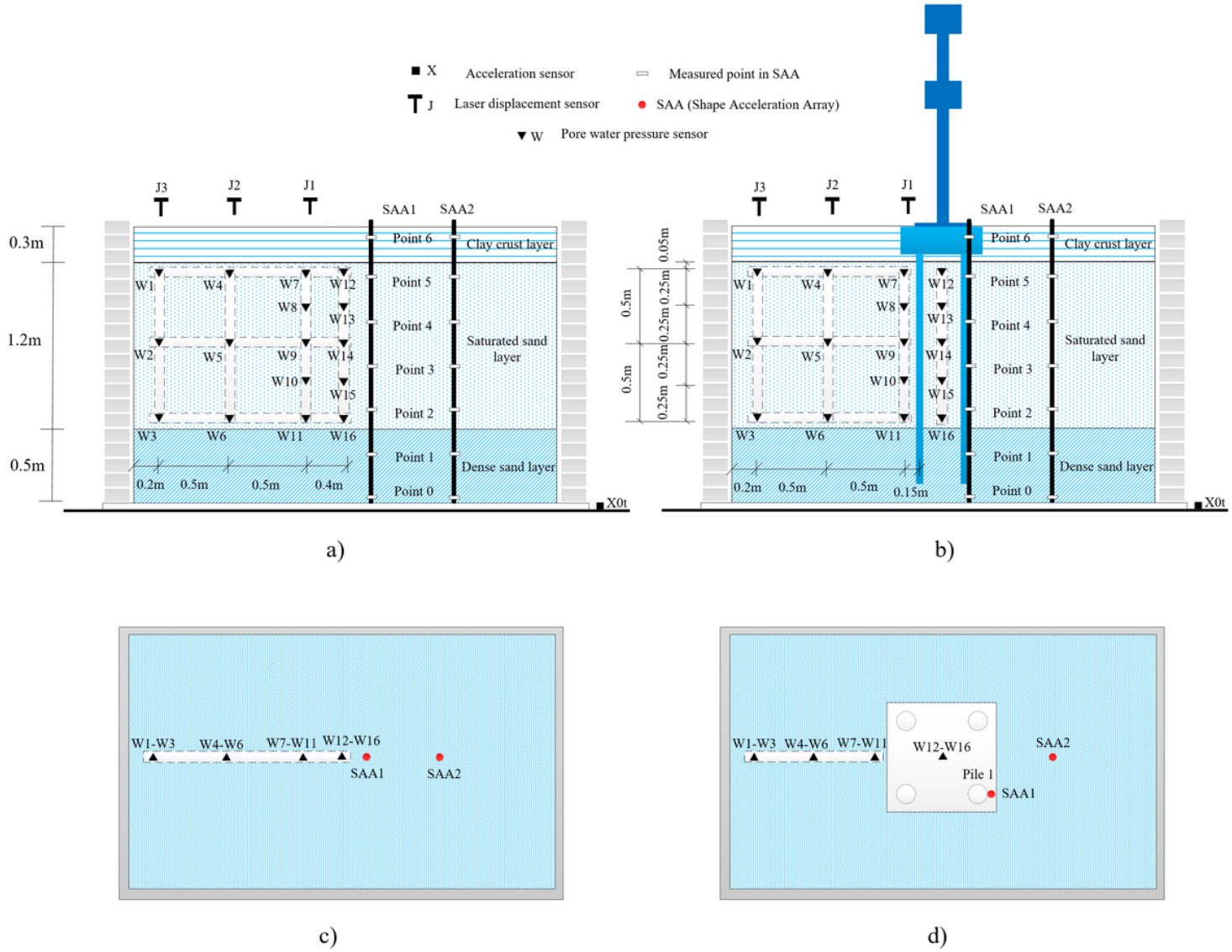

Figure 3

Layout of test package and instrumentation: a) elevation view of free field; b) elevation view of non-free field; c) plan view of free field; and d) plan view of non-free field

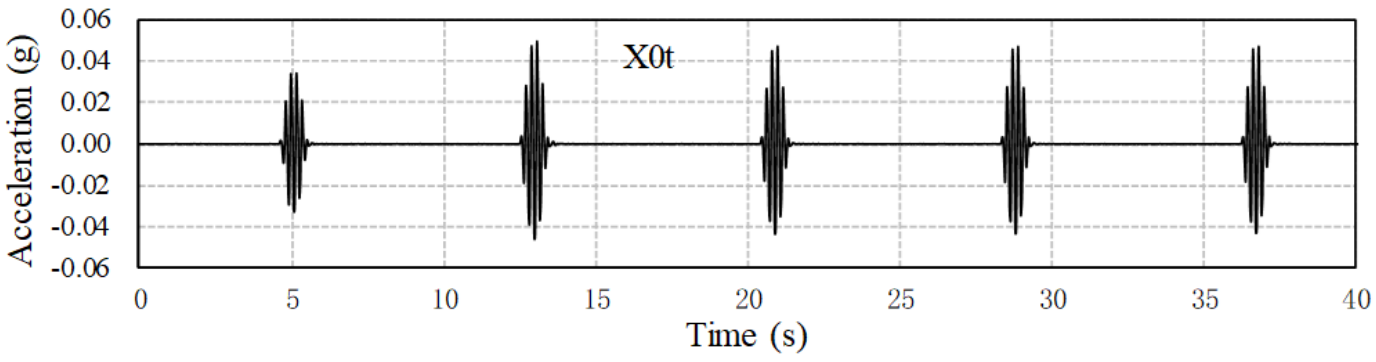

Figure 4

Sine beat wave acceleration time history measuring by X0t

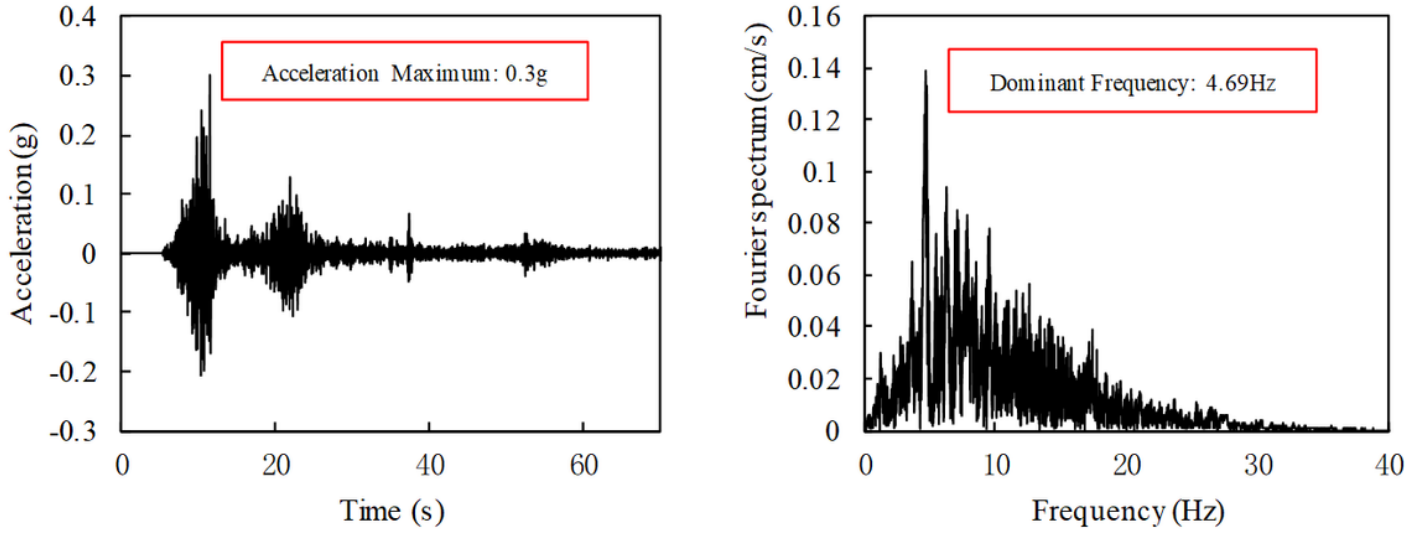

Figure 5

Acceleration time history and corresponding Fourier spectra of Wolong ground motion record in Wenchuan Earthquake

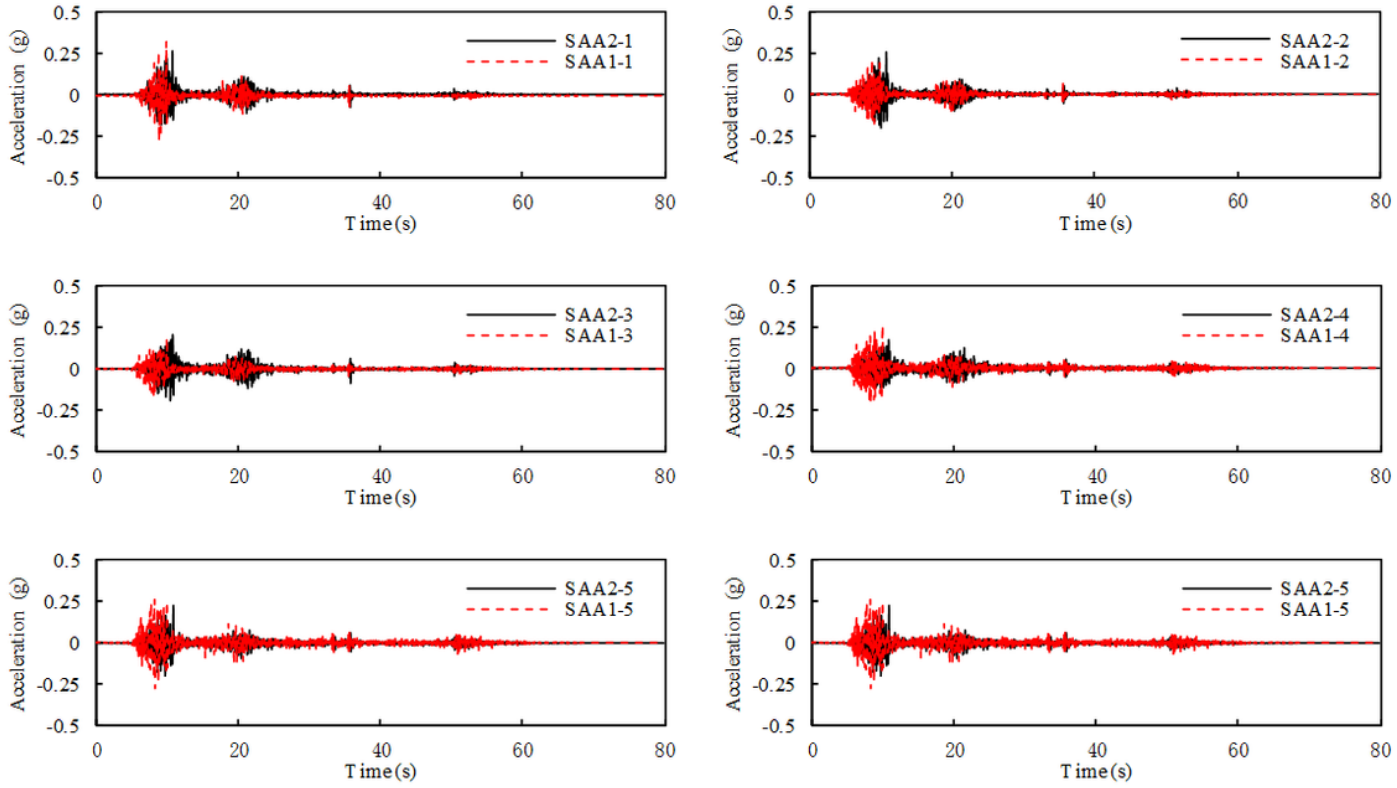

Figure 6

Acceleration time histories of pile and soil in NF Experiment for 0.3g Wolong ground motion record

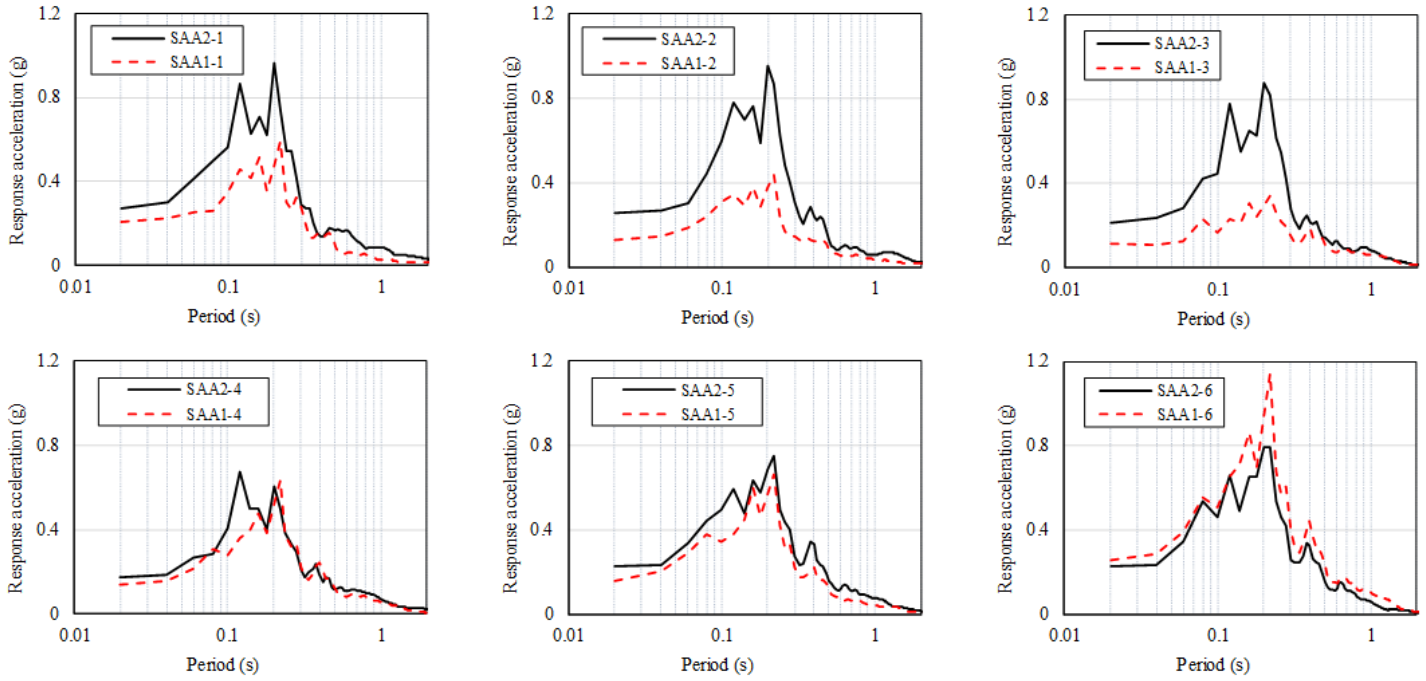

Figure 7

Response spectra of pile and soil in NF Experiment for 0.3g Wolong ground motion record

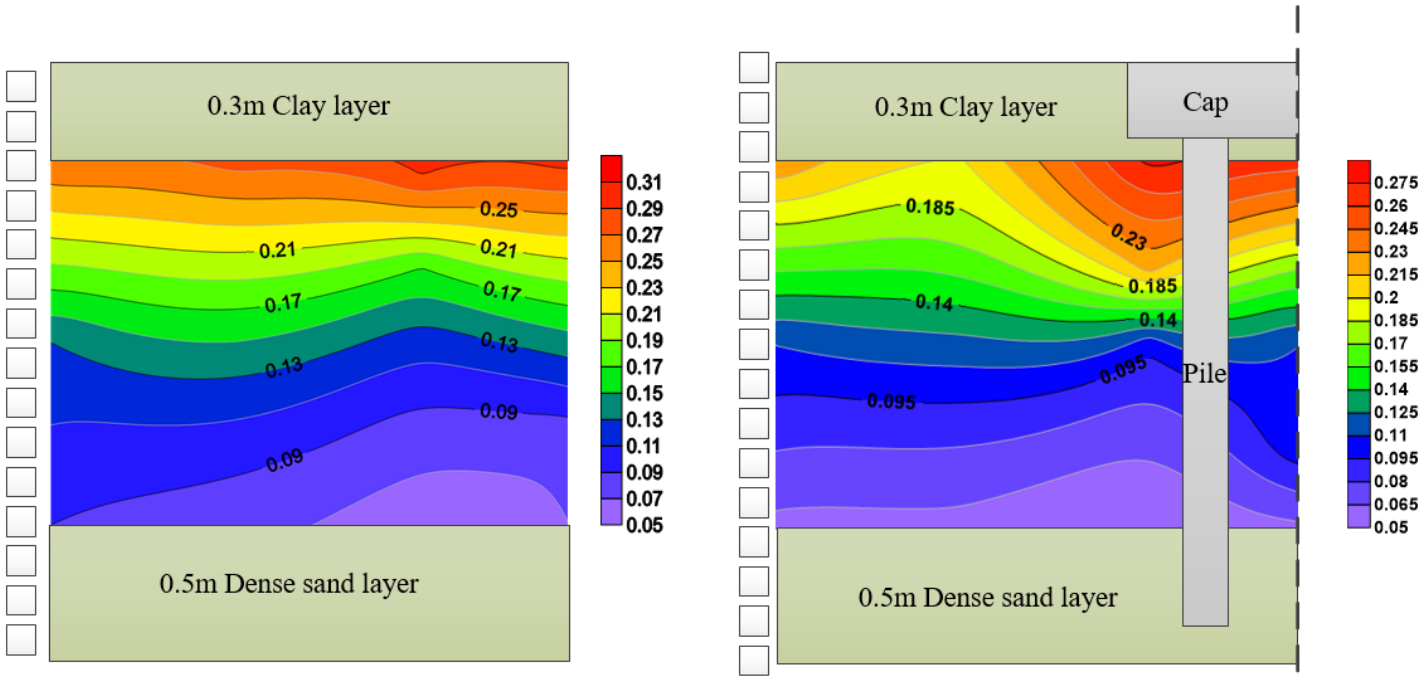

Figure 8

Peak porewater pressure color nephograms for 0.05g sine beat wave in: a) Experiment-F; b) Experiment-NF

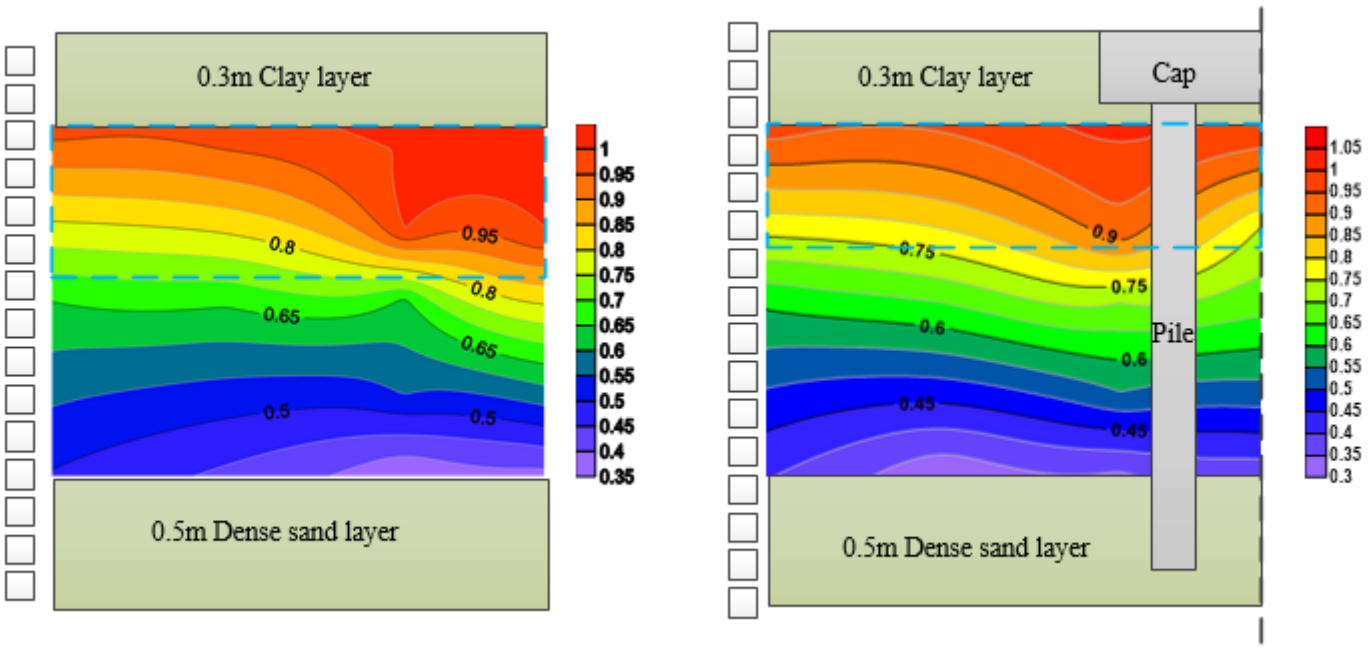

Figure 9

Peak porewater pressure color nephograms for 0.3g Wolong ground motion record in: a) Experiment-F; b) Experiment-NF

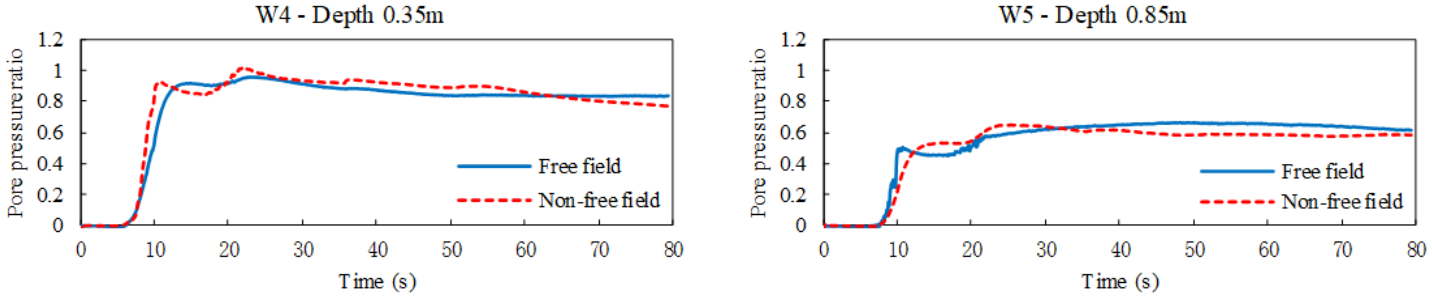

Figure 10

Porewater pressure time histories at measuring points W4 and W5 (away from the structures or soil center)

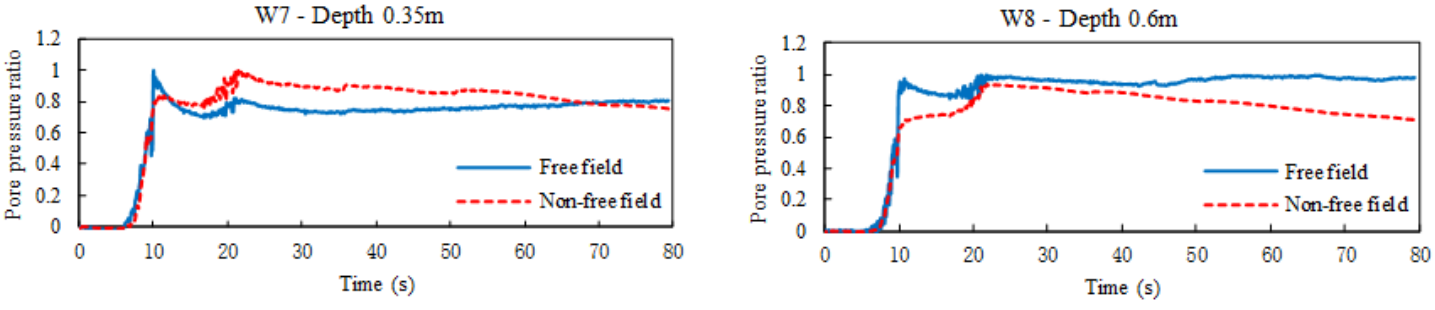

Figure 11

Porewater pressure time histories at measuring points W7 and W8 (near the structures)

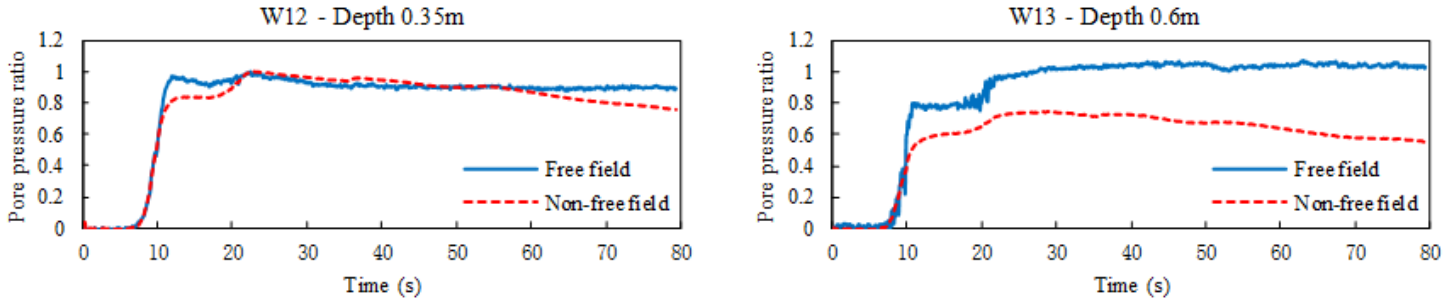

Figure 12

Porewater pressure time histories at measuring points W12 and W13 (at the soil center or under the cap)

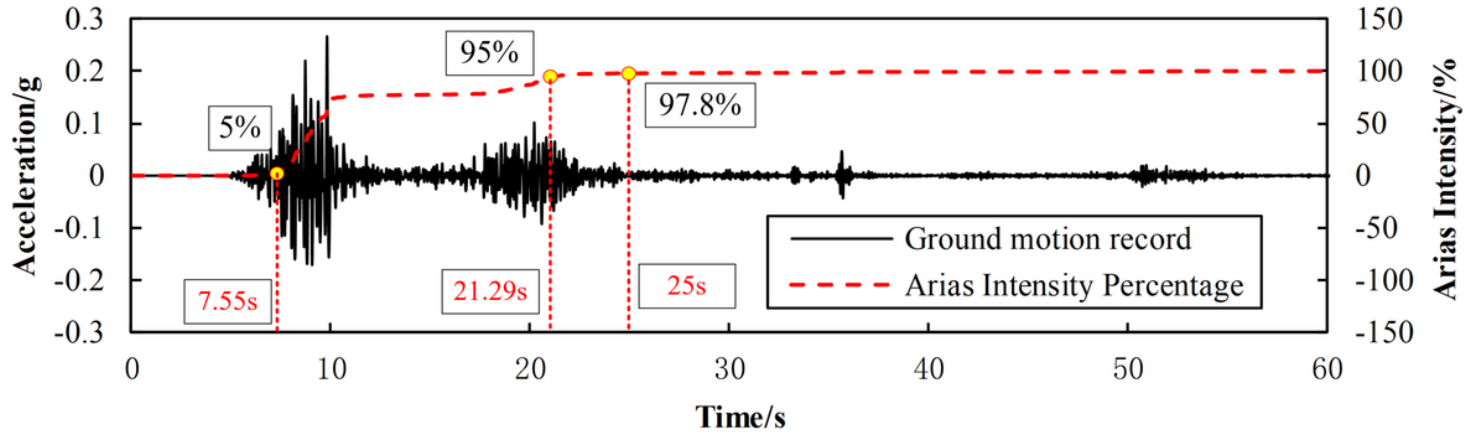

Figure 13

Acceleration data measured at X0t and the corresponding Arias Intensity curve

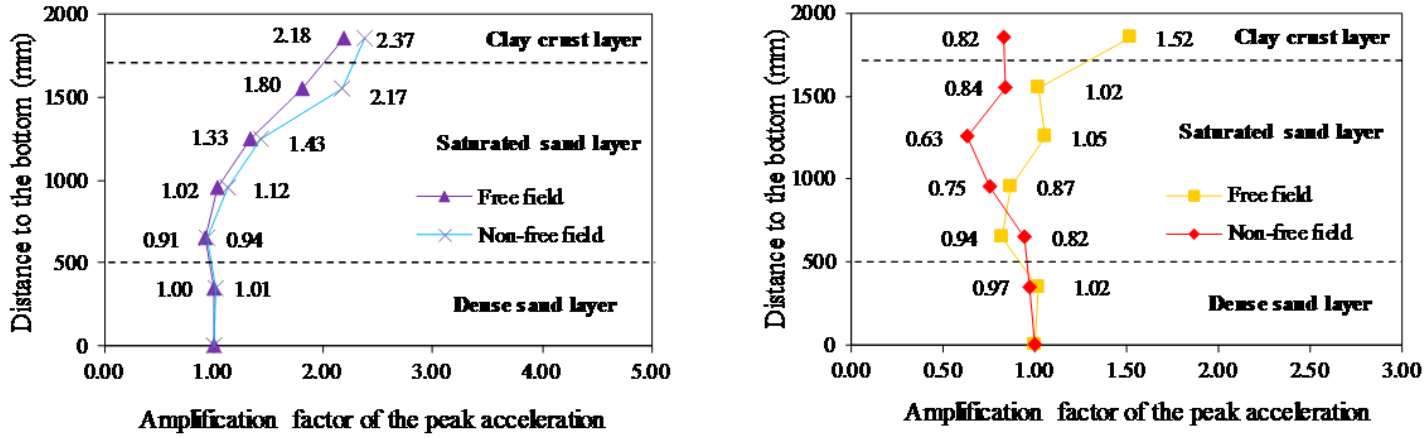

Figure 14

Amplification factors of peak acceleration from SAA2 in both experiments for: a) 0.05g sine beat wave; b) 0.3g Wolong ground motion record

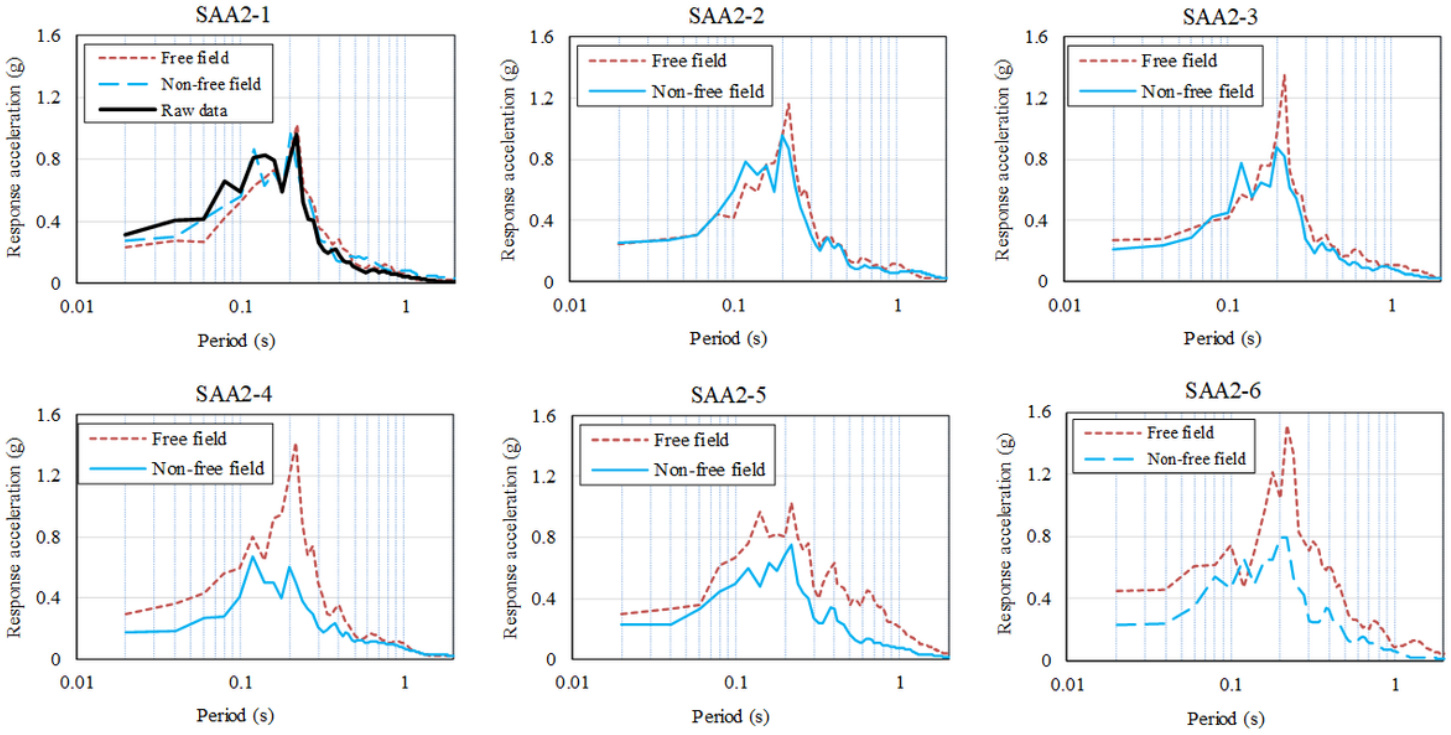

Figure 15

Acceleration response spectra at SAA2 measuring points and raw data for 0.3g Wolong ground motion record

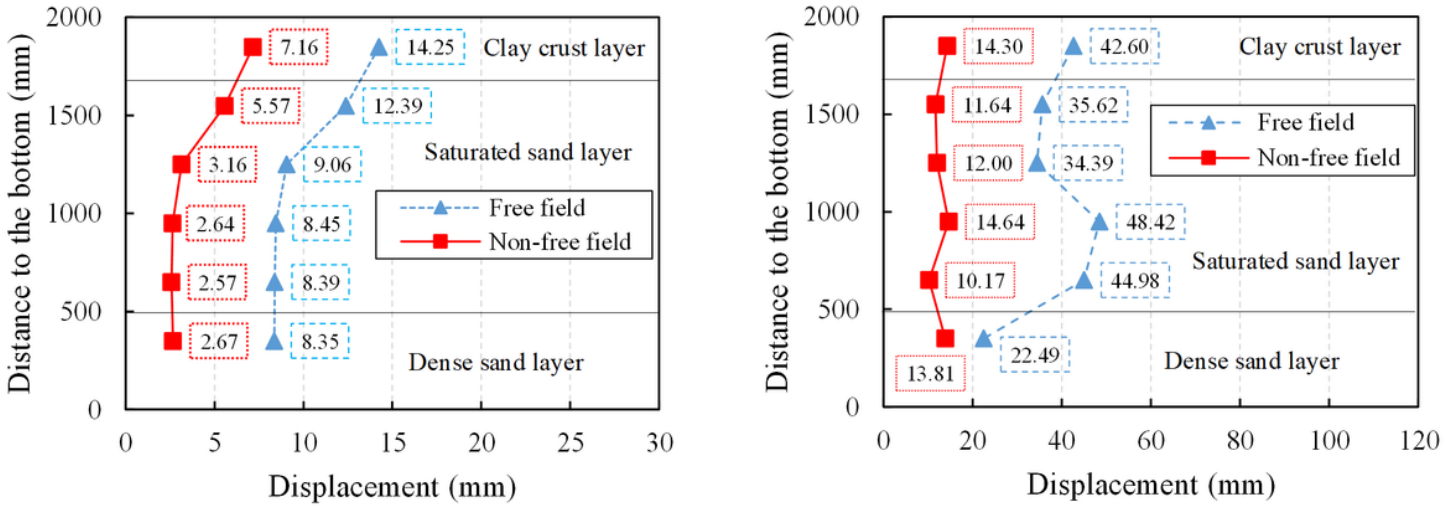

Figure 16

Amplitude of lateral displacements of soils at SAA2 measuring points in both experiments for: a) 0.05g sine beat wave; b) 0.3g Wolong ground motion record